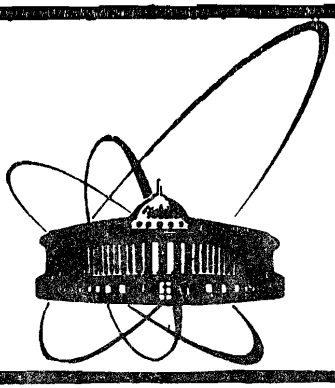

объединенный
институт
ядерных
исследований
дубна

E6-86-233

Yu.P.Gangrsky, Han Gyong I, K.P.Marinova,
B.N.Markov, E.G.Nadjakov, Tran Cong Tam

LOW AMOUNT NUCLIDE REGISTRATION BY AN ATOMIC BEAM LASER SPECTROMETER

Submitted to "Nuclear Instruments
and Methods in Physics Research A"

1986

The investigations of hyperfine structure, isotope and isomere shifts of atomic optical spectra yield information about mechanic, electric and magnetic moments of long and short lived nuclear states. Contemporary optical facilities are based on the application of dye lasers. Their high power and spectral resolution with the possibility of broad band frequency tuning led recently to the development of various optical methods in nuclear physics with good resolution, selectivity with respect to Z and A , high efficiency and sensitivity, and the possibility of investigating short lived nuclear states /1-3/.

1. Laser specrtometer

The technique of a mass separated evaporated atomic beam, intersected by a tunable dye laser ray, and registering the fluorescence light, is known /4,5/. Such type of technique, but trying to apply it without mass separation, by making use of the laser spectroscopy own sensitivity, has been developed in Dubna and described in more detail elsewhere /6/.

Our technique is based, firstly, on the atomic beam evaporated from an oven with collimator; secondly, on the ray of a tunable ring dye laser Spectra Physics (SP) 380 A scanning the frequency in a range up to 30 GHz for a time 0.1 s to 10 min; and thirdly, on the resonance fluorescence light focused by a lens system on a photomul-

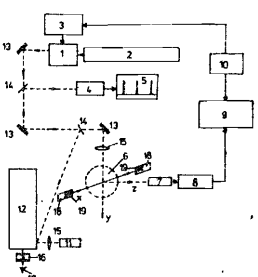

Fig.1. Laser spectrometer: 1. dye laser Spectra Physics (SP) 380 A with a maximum output 800 mW at R6G and input power 4 W; 2. Ar ion laser SP 171-18 with maximum multi-line power 24 W; 3. scanning electronics SP 476; 4. scanning interferometer SP 470 ; 5. oscilloscope; 6. interaction region: atomic beam (x), laser ray (y), fluorescence light (z); 7. photomultiplier FEU 79 ; 8. amplification and discrimination system; 9. 1024 channel analyzer ICA 70 ; 10. trigger generator; 11. hollow cathode etalon lamp; 12. spectrograph DFS 8 ; 13. mirror; 14. ray splitter; 15. lens; 16. ocular; 17. eye; 18. oven; 19. collimator.

tiplier, operated in single photon counting mode, coupled to a multichannel analyzer scanning 10^3 channels synchroniously with dye laser frequency tuning with a width up to 30 MHz per channel. The atomic beam, the laser ray and the fluorescence light intersect each other under 90 degrees in a 6 mm^3 interaction region: see fig. 1.

The atoms are evaporated in a Ta oven heated up to 600 - 1800 K for a time of 30 s . The atomic beam is collimated with an efficiency (for definition: see sect. 3) of 3×10^{-4} (low) or 2×10^{-3} (high).

To achieve the single photon counting mode a selection of a suitable exemplar of a FEU 79 photomultiplier with well developed one-, two- and so on photon peaks in the electron pulse amplitude distribution and a suitable choice of the discrimination level has been performed. The registration efficiency (for definition see sect. 3) consists of photon production efficiency: in our case of odd isotopes with many line components it is about 2×10^{-1} , and of photon detection efficiency, consisting of two nearly equal parts: light collection and photomultiplier counting: altogether about 5×10^{-3} ; it should be multiplied by the interference filter transmission 2.5×10^{-1} (when used: see below).

The ultrahigh vacuum chamber is capable to be evacuated down to about 10^{-10} Torr, but was operated at a high vacuum of 10^{-6} Torr, achieved for about 30 min.

Special measures have been taken to reduce oven light background by suitable diaphragms, and also by introducing an interference filter before the photomultiplier for the 5765.20 A line with a maximum transmission at 5768 Å and a band width of 75 Å , experimentally reducing the efficiency additionally 4 times, but also reducing the oven background to effect ratio about 10^2 times. Also special diaphragms to reduce laser light background have been introduced. Attention has been paid to reduce photomultiplier darkness noise by keeping it long enough lightproof with voltage implied, and by choice of the electronics parameters. Noise induced via the electrical set has been eliminated too.

The so achieved photomultiplier noise in our case is 40 count/s , the laser background 2500 count/s at 100 mW laser ray power, and the oven background: 500 count/s at an oven sample temperature 1350 K corresponding to an oven heater temperature of about 1750 K.

2. Resolution and selectivity

A compromise between resolution and efficiency led us to accept

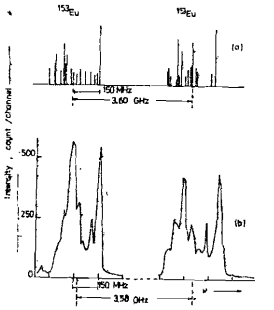

Fig.2. Spectra of the $^{151, 153}Eu$ I 5765.20 Å line: (a) ref. /7/ with frequency stabilization and resolution 3 MHz; (b) our results without frequency stabilization and resolution 30 MHz.

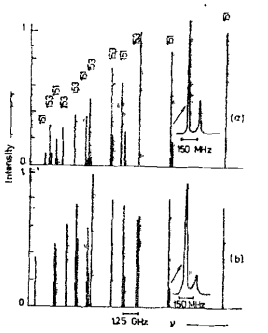

Fig.3. Spectra of the $^{151, 153}Eu$ I 6018.19 Å line: ^{63}Eu (a) obtained under collaboration in Moscow; (b) obtained in Dubna.

for the moment a Doppler broadening of about 25 MHz (see next sect. 3). The laser line width is 20 MHz . This results in a total hyperfine structure line component width (resolution) of about 30 MHz . It is about one order of magnitude worse than the best known measurements /7/ on the ^{63}Eu I 5765.20 Å line from the $4f^7 6s^2\ a^8S^o_{7/2} \longrightarrow 4f^7 6s6p\ z^6P_{7/2}$ transition: see comparison in fig. 2. However it is of the same order of magnitude as the recently applied to other ^{63}Eu lines /8/, and is sufficient to resolve nearer to normal broader hyperfine structure, e.g., the ^{63}Eu I 6018.19 Å line from the $4f^7 6s^2\ a^8S^o_{7/2} \longrightarrow 4f^7 6s6p\ z^8P_{9/2}$ transition: see fig. 3. Considerably better Doppler width is planned for the improved dye laser SP 308 D with the Stabilok reference interferometer and electronic frequency stabilization system. It will reduce the laser line width to 1 MHz , allowing a reduction of the Doppler broadening to 2.5 MHz , and thus a better resolution of 3 MHz .

There is no question about the selectivity with respect to Z due to the immense distance between the lines of different elements. One could be tempted to say that the selectivity with respect to A is also good enough since, as one can see from figs. 2 and 3, the distance between lines or line components of different isotopes is large enough as compared to the line or line component width. However, near to the basic laser line there are laser modes which can be minimized but not completely avoided. In our case they remained on the level 2×10^{-4} of the basic line after best laser adjust-

ment. If there is some contamination of another A and the same Z in the sample, satellites of its hyperfine structure appear at frequencies near to this of its neighbouring isotope line. It follows from the above estimation that the contaminating isotope should not be more than 20 times the measured one (see sect. 4 and its fig. 5). It means that in a 100 mg sample with $A \approx 150$ and 4×10^{20} atom, where the measured, e.g., radioactive isotope contains 10^{12} atom or a concentration 2.5×10^{-9}, the contaminating, e.g., stable isotope should not exceed 2×10^{13} atom or a concentration 5×10^{-8} of the basic sample isotope.

3. Efficiency and sensitivity

To determine the Doppler broadening, efficiency and sensitivity parameters, one needs to know the flux of evaporated atoms calculated theoretically, and the photon counting velocity determined experimentally.

The calculation concerns also the atomic beam collimation and is based on a method by one of us described elsewhere [9]. In short, this method uses the Maxwell velocity distribution in the oven and an empirically based hypothesis about atom scattering from collimator walls, determining the collimator transmission. The starting quantities are the atomic vapour density in the oven n and the Maxwell velocity v :

$$n = P/kT \quad , \qquad v = \sqrt{2kT/M} \tag{1}$$

derived from empirical tables of vapour pressure P [Pa] at a given experimentally measured absolute temperature T [K] [10]. It yields, in principle, the whole space $(\vec{r})$ and velocity $(\vec{v})$ distributions of the atomic flux out of the oven.

In practice we have calculated the Doppler line width at 1/2 height $\Delta\nu$ (used in previous sect. 2), and the integral quantities (to be used further in this sect. 3) χ [atom] : the local number of atoms in the interaction region; φ [atom/s] : the local flux (number per second) of atoms intersecting the cross section of the interaction region perpendicular to the atomic beam axis; Ψ [atom/s] : the total flux of atoms evaporated from the oven in all directions; (χ , φ , Ψ) are denoted generally by θ .

The main sources of error are related: 1) to possible chemical changes of the sample and/or its surface layer, changing P , 2) to the empirical data about P(T) , varying in some cases more than one

order of magnitude between different tables, and 3) to the possibility that the effective T is located at another place than the measured one. The first source has been found not to act above a given temperature T (see sect. 4, 6). To eliminate the second and third error sources we have made weight measurements of the total evaporated quantity for several hours $\int \Psi dt$ and compared it with the calculated one, the difference corresponding to a temperature change of 12.5 K only. We have checked also the space width of the atomic flux by comparing the experimental data of ref. [11] with our theoretical width [9] giving a better fit than the one of ref. [11] itself.

The necessary experimental quantities are as follows: N_e [count/s] is the effect, meaning number of counts per second in the peak of the hyperfine structure over background; N_b [count/s] , the background, both corrected for counting system total dead time and for eventual deviations from single photon counting [12]; a , the minimal ratio of the effect to the effect plus background statistical error, for which the effect is accepted to be observable, in our case we assume $a = 3$; and t_c [s] , the measuring time per channel.

The general definition, determination and prognosis of resolution, efficiency and sensitivity parameters are discussed by one of us elsewhere [12]. We remind shortly the particular practically used definitions here. We introduce the reciprocal efficiency parameters (χ_e , φ_e , Ψ_e) denoted generally by θ_e , as follows:

$$\theta_e = \theta / N_e \cdot \tag{2}$$

We notice that in the limit when background is negligible, the reciprocal sensitivity parameters (χ_s , φ_s , Ψ_s) or generally θ_s , limited by statistics, are directly related to efficiency and time only:

$$\theta_s = a^2 \theta / (N_e \cdot t_c) = a^2 \theta_e / t_c \cdot \tag{3}$$

In the opposite limit when background, as usual, is high enough, the reciprocal sensitivity parameters limited by background are related not only to efficiency and time, but also to background:

$$\theta_s = a\,\theta \sqrt{N_b t_c} / (N_e t_c) = a\,\theta_e \sqrt{N_b / t_c} \cdot \tag{4}$$

Let us notice that the total reciprocal efficiency, evaporated atoms per count in the peak, is Ψ_s , its part due to collimation is

$\varphi_e/\varphi_e = \psi/\varphi$ and to registration is φ_e . The total reciprocal sensitivity, minimal observable total flux of evaporated atoms, is ψ_s ; and its part due to registration, minimal observable local flux of atoms passed through interaction region cross section, is φ_s . Another accepted way to define registration reciprocal sensitivity, minimal observable number of atoms in interaction region volume, is χ_s .

4. Pure natural Eu

The dependence of efficiency and sensitivity on flux and temperature is shown in fig. 4. As it should be, efficiency is not changed when changing flux by many orders of magnitude. However, this is true after an initial sample heating to remove oxide coating, not to be seen in the figure. Sensitivity becomes worse at very high temperatures, due to increased background.

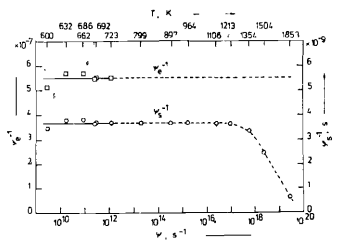

Fig.4. Dependence of total efficiency ψ_e^{-1} (squares) and total sensitivity ψ_s^{-1} (circles) on total flux φ (for one of both natural $_{63}Eu$ isotopes) and sample temperature T ; dependence $\varphi(T)$: from fig. 6 of ref. /9/. Real experiment (solid lines), and extrapolation to higher φ , T (dashed lines) by means of background N_b dependence on T /12/. Normalized to standard parameters: second row of table 2.

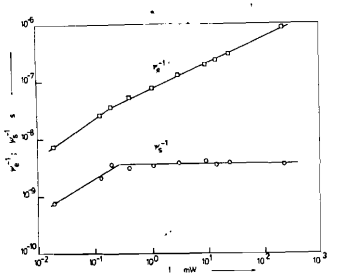

Fig.5. Dependence of total efficiency ψ_e^{-1} (squares) and total sensitivity ψ_s^{-1} (circles) on laser power I . Normalized to standard parameters: second row of table 2, except: T = 600 - 1200 K (no oven background).

The dependence of efficiency and sensitivity on laser power is shown in fig. 5. One can see that ψ_e^{-1} , and also N_e , tends to be nearly proportional to I only at low I , but is proportional to $\sqrt{I}$ at higher I . Since N_b becomes constant due to darkness noise at lowest I , but is proportional to I at low and high I ,

ψ_s^{-1} is nearly proportional to $\sqrt{I}$ at low I (probably tending to proportionality to I at lowest I), and becomes constant at higher I .

Saturation of N_e and thus ψ_e^{-1} with I is expected at high I due to optical pumping to different ground state sublevels in odd nuclei as those studied here. It results in a number of transitions per atom during its 4 μs long flight through the 1 mm thick interaction region not higher than, e.g., 1.25 . This is in contrast to the case of even-even nuclei with radiation time, e.g., $\approx 4 \times 10^{-8}$ s , where multiple radiation could follow which would increase the saturation efficiency in the accepted case 80 times. In any case, at saturation the effect N_e will depend on the local flux φ and thus on the interaction region cross section (surface dependence), but when we are still far from it: on the local number χ and thus on the interaction region volume (volume dependence). However fig. 5 shows that complete saturation is not reached in our case, possibly due to the broad laser line in combination with optical pumping.

Table 1

Reciprocal efficiency (χ_e , φ_e , ψ_e) and sensitivity (χ_s , φ_s , ψ_s) parameters dependence on experiment at sample temperature T , laser power I (time t_c = 1 s and low collimation) for pure natural $_{63}Eu$

Experiment	T, K	I, mW	χ_e, s	φ_e	ψ_e	χ_s	φ_s, s^{-1}	ψ_s, s^{-1}
1	675	~60	2.767×10^{-2}	1.081×10^{4}	3.599×10^{7}	2.780×10^{0}	1.086×10^{6}	3.616×10^{9}
2	635	215	1.896×10^{-2}	6.422×10^{3}	2.139×10^{7}	4.881×10^{0}	1.848×10^{6}	6.155×10^{9}
3	667	139	3.040×10^{-2}	1.180×10^{4}	3.929×10^{7}	5.045×10^{0}	1.958×10^{6}	6.521×10^{9}
4	636	136	2.279×10^{-3}	8.637×10^{2}	2.876×10^{6}	3.754×10^{-1}	1.423×10^{5}	4.738×10^{8}

Table 2

Reciprocal efficiency (χ_e , φ_e , ψ_e) and sensitivity (χ_s , φ_s , ψ_s) standard parameters for time $t = t_c$ and indicated collimation (at oven sample temperature T = 1350 K corresponding to oven heater temperature about 1750 K , laser ray power I = 100 mW)

t, s	Collimation	χ_e, s	φ_e	ψ_e	χ_s	φ_s, s^{-1}	ψ_s, s^{-1}
1	low	8.907×10^{-3}	3.395×10^{3}	1.131×10^{7}	1.463×10^{0}	5.578×10^{5}	1.858×10^{9}
1	high	8.907×10^{-3}	3.395×10^{3}	1.817×10^{6}	1.463×10^{0}	5.578×10^{5}	2.985×10^{8}
0.01	low	8.907×10^{-3}	3.395×10^{3}	1.131×10^{7}	1.463×10^{1}	5.578×10^{6}	1.858×10^{10}
0.01	high	8.907×10^{-3}	3.395×10^{3}	1.817×10^{6}	1.463×10^{1}	5.578×10^{6}	2.985×10^{9}

The dependence of all efficiency and sensitivity parameters on experiment is shown in table 1. Their variation is due to random factors such as changes in: 1) atomic beam direction, 2) laser ray direction, 3) photomultiplier pulse amplitude (all three leading to changes in effect and background), 4) thermocouple fixation (changes in effect), 5) vacuum (changes in background, due to the laser and oven light scattering by chamber residual gas).

By taking geometric average values of experiments 2-4 (1 has been done with another photomultiplier) with a double weight to optimal experiment 4 , and by accepting as standard conditions T = 1350 K (higher temperature necessary for admixture evaporation: see sect. 6) I = 100 mW , the standard parameters, shown in table 2 for two values of time t and two collimations, have been obtained. Let us notice that the reported best level of registration reciprocal sensitivity χ_s = 1 atom and $\psi_s = 10^6$ atom/s for odd isotopes of the rare element region [2, 3] has been reached. A total reciprocal sensitivity on the level $\psi_s = 5 \times 10^8$ atom/s is good enough.

5. Evaporation laws

The registration of small amounts of $_{63}$Eu in samples of other elements may present some surprises due to peculiarities in the evaporation process. Therefore samples of $_{62}$Sm and $_{60}$Nd contaminated with $_{63}$Eu on the concentration level $c \approx 10^{-4}$ [Eu atom per sample atom] have been studied and the validity of vapour pressure law over ideal solutions checked. This hypothetic law states that Eu vapour concentration, instead of n over pure Eu, will become cn over the Sm or Nd sample. Correspondingly the θ quantities of sect. 3 will be changed to $c\theta$.

Firstly, we introduce the theoretical evaporation law for the concentration c(t) variation with time t :

$$c_t(t) = c \exp\left[-\int_0^t (\psi/\delta)\,dt\right] ; \qquad \psi = \psi^{Eu\ in\ X}, \quad \delta = \delta^{Eu\ in\ X}, \quad (5)$$

where $c = c_t(0)$ is the initial concentration; ψ , the total flux of one of both ^{151}, $^{153}_{63}$Eu isotopes from the sample; and δ , the number of this isotope atoms in the sample X = Sm, Nd . Actually (5) is valid if the Eu concentration is low and the sample element X evaporates little during the process time t . In this case, with the ideal solution hypothesis, ψ and δ can be changed to the same quantities ψ^{Eu} and δ^{Eu} for a pure Eu sample with the same total number of atoms. We are going to use (5) in the last form. In the contrary case the concentration $c_t(t)$ must be changed to the considered $_{63}$Eu isotope number of atoms $\delta = \delta(t)$; and c , to $\delta(0)$.

Secondly, we propose an ideal experimental evaporation law:

$$c_i(t) = \theta_e^{Eu} / \theta_e^{X} ; \qquad \theta_e^{X} = \theta^{Eu} / N_e^{Eu\ in\ X} \quad (6)$$

which measures actually the ratio of Eu vapour concentration over the sample X to that of saturated vapour over pure Eu . It should be valid for the Eu sample concentration too, if the ideal solution hypothesis would be true. The difference in $c_i(t)$ between the case $\theta = \chi$ and $\theta = \psi$ (the second one identical with the case $\theta = \Psi$) is related to the difference between volume (no excitation saturation) and surface (excitation saturation) dependence of the effect N_e on number χ , respectively flux ψ of atoms, discussed in the previous sect. 4. In our intermediate case, having in mind their small difference, we just take the arithmetic average value of $c_i(t)$ for $\theta = \chi$ and $\theta = \psi$.

And thirdly, we deduce the real experimental evaporation law:

$$c_r(t) = \int_t^\infty N_e \psi_e^{Eu}\,dt \Big/ \delta^{Eu} ; \qquad N_e = N_e^{Eu\ in\ X} \quad (7)$$

for the actual Eu sample concentration. We normalize (5) to experiment (7) by assuming $c = c_r(0)$.

6. Natural Eu admixtures in Sm and Nd

The results for all the three evaporation laws and for two experiments with $_{63}$Eu in $_{62}$Sm are presented in fig. 6; and with $_{63}$Eu in $_{60}$Nd , in fig. 7. Each admixture experiment is treated with the data θ_e^{Eu} of the suitable pure Eu experiment: Sm (1) with row 1; Sm (2), Nd (1, 2) with row 4 of table 1. In all the experiments the temperature T has been increased to maximum for a time t_o (several tens or hundreds of seconds) and then kept almost unchanged.

One can see in figs. 6 and 7 a different behaviour of the evaporation curves in the three time t intervals $(0,t_i)$, (t_i,t_f), (t_f,∞), where t_i is related to t_o being near to it, and t_i ,

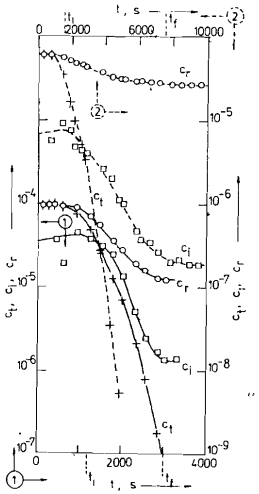

Fig.6. Time (t) dependence of three natural $_{63}Eu$ in $_{62}Sm$ concentrations: theoretical (5) $c_t(t)$ (crosses), ideal experimental (6) $c_i(t)$ (squares), real experimental (7) $c_r(t)$ (circles); for two experiments (1: solid lines, 2: dashed lines). The middle fast decrease interval end points t_i, t_f for each experiment are also indicated: see text sect.6.

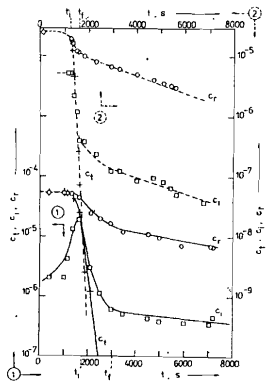

Fig.7. Time (t) dependence of three natural $_{63}Eu$ in $_{60}Nd$ concentrations. The rest as for fig. 6.

t_f are defined below. In $(0,t_i)$ the theoretical concentration $c_t(t)$ decreases slowly due to the low temperature T and thus flux Ψ. The ideal concentration $c_i(t)$, measuring actually a relative evaporation velocity, is lower, almost constant and even increases in some cases, probably due to oxide coating evaporation hindrances and to its removal with time and temperature. The real concentration $c_r(t)$ decreases slower than $c_t(t)$ due to both reasons mentioned above: low flux and low evaporation velocity. In (t_i,t_f) a fast approximately exponential decrease of all three $c_t(t)$, $c_i(t)$, $c_r(t)$ is observed, due to almost constant T, with exponential constants differing not very much if the slow exponentials of $c_i(t)$, $c_r(t)$ in (t_f,∞) are subtracted. The ideal law is approximately valid, the evaporation velocity being limited almost only by collimation. In (t_f,∞) $c_t(t)$ continues to decrease according to the same exponential. However both $c_i(t)$, $c_r(t)$ follow another exponential with a much lower constant. The relative evaporation velocity $c_i(t)$ remains correspondingly below the integral concentration $c_r(t)$.

This is an indication that the ideal law is violated here, and evaporation is limited by something stronger than collimation, e.g., by slow diffusion of Eu from sample interior to its surface.

As one can see from (6), the reciprocal efficiency $c_i\theta_e$ and sensitivity $c_i\theta_s$ for $_{63}Eu$ in $_{62}Sm$ and $_{60}Nd$ remain the same as the accepted ones from the corresponding pure Eu experiment. However the effective reciprocal sensitivity $c_r\theta_s$ can be different due to other conditions, e.g., temperature T (changing N_b), power I (changing N_e, N_b), and also due to other evaporation velocity (changing N_e). In table 3 we give two concentrations of natural $_{63}Eu$: the initial one c at time $t = 0$, and the residual one c_m at a later time $t = t_m$, coinciding with the time of one of the first measurements, defined as follows:

$$c = c_r(0), \qquad c_m = c_r(t_m) \qquad [c_i(t_m) = max]. \tag{8}$$

We give also the absolute numbers of atoms of one of both $_{63}Eu$ isotopes: δ corresponding to c, and δ_m corresponding to c_m. At last, the reciprocal sensitivities $c_m\theta_s = (c_m\chi_s, c_m\varphi_s, c_m\psi_s)$ at $t = t_m$ are shown.

Table 3

Concentrations (c, c_m), numbers of atoms (δ, δ_m): see text sect. 6; effective reciprocal sensitivity $(c_m\chi_s, c_m\varphi_s, c_m\psi_s)$ at temperature T, power I (time $t_c = 1$ s, high collimation) for natural $_{63}Eu$ admixtures in $_{62}Sm$ and $_{60}Nd$

Sample	Experiment	c	c_m	δ	δ_m	T, K	I, mW	$c_m\chi_s$	$c_m\varphi_s, s^{-1}$	$c_m\psi_s, s^{-1}$
Sm	1	9.607×10^{-5}	9.607×10^{-5}	3.642×10^{16}	3.642×10^{16}	1200	~60	1.612×10^{0}	6.987×10^{5}	3.740×10^{8}
Sm	2	6.098×10^{-5}	6.098×10^{-5}	2.867×10^{16}	2.867×10^{16}	1150	5.75	3.361×10^{-1}	1.544×10^{5}	8.261×10^{7}
Nd	1	5.457×10^{-5}	4.516×10^{-5}	2.282×10^{16}	1.889×10^{16}	1300	6.05	1.974×10^{0}	1.023×10^{6}	5.475×10^{8}
Nd	2	2.453×10^{-5}	1.592×10^{-5}	1.225×10^{16}	7.951×10^{15}	1350	4.85	9.584×10^{0}	5.297×10^{6}	2.835×10^{9}

Table 4

Concentrations $(\Delta c, \Delta c_m)$, numbers of atoms $(\Delta\delta, \Delta\delta_m)$: see text sect. 7; effective reciprocal sensitivity $(\Delta c_m\chi_s, \Delta c_m\varphi_s, \Delta c_m\psi_s)$ at temperature T, power I (time $t_c = 1$ s, high collimation) for mass separated $^{153}_{63}Eu$ implanted in $_{42}Mo$ and $^{151}_{63}Eu$ implanted in $_{73}Ta$

Sample	Isotope	Δc	Δc_m	$\Delta\delta$	$\Delta\delta_m$	T, K	I, mW	$\Delta c_m\chi_s$	$\Delta c_m\varphi_s$ s^{-1}	$\Delta c_m\psi_s$ s^{-1}
Mo	^{153}Eu	1.118×10^{-6}	7.143×10^{-7}	1.186×10^{14}	7.577×10^{13}	1500	8.65	9.173×10^{1}	5.318×10^{7}	2.846×10^{10}
Ta	^{151}Eu	7.442×10^{-7}	4.012×10^{-7}	3.343×10^{13}	1.802×10^{13}	1850	112.5	4.500×10^{1}	2.908×10^{7}	1.556×10^{10}

One sees that concentrations c from different experiments are roughly the same, as they should be up to the variations discussed in sect. 4. One observes also that up to these variations, sensitivities in table 3 are the same as the standard ones derived from pure Eu experiments in table 2. It means that: 1) real experimental conditions of table 3 do not make an essential difference from the standard ones accepted in table 2; 2) evaporation of Eu out of Sm and Nd is not considerably hindered.

7. Mass separated Eu implanted in Mo and Ta

Preliminary results are reported, and one of the spectra is shown in fig. 8. One sees the 100 times predominant presence of implanted $^{153}_{63}Eu$ over residual natural admixture $^{151}_{63}Eu$.

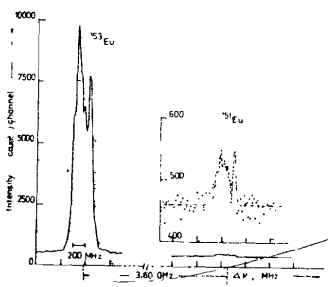

Fig.8. Spectra of the $^{153}_{63}Eu$ I implanted in $_{42}Mo$ 5765.20 Å line at evaporation start. The residual $^{151}_{63}Eu$ line is also observed with 1% intensity.

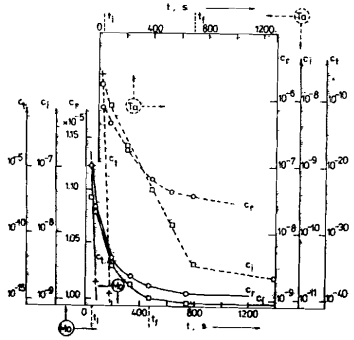

Fig.9. Time (t) dependence of three concentrations of mass separated $^{153}_{63}Eu$ implanted in $_{42}Mo$ (solid lines) and $^{151}_{63}Eu$ implanted in $_{73}Ta$ (dashed lines). The rest as for fig. 6.

Time dependence experiments on mass separated $^{153}_{63}Eu$ implanted in $_{42}Mo$ and $^{151}_{63}Eu$ implanted in $_{73}Ta$ are shown in fig. 9. No first region $(0, t_i)$ is observed here at variance from figs. 6 and 7, possibly due to the immediate temperature rise ($t_0 \approx 30 - 45$ s) here to very high values. There is a second (t_i, t_f) fast evaporation region which seems to be related to the implanted isotope of $_{63}Eu$.

There is also a third (t_f, ∞) slow evaporation region, possibly due to natural admixture $_{63}Eu$. In fact, in the last case the $_{63}Eu$ isotope being earlier implanted, and the other one being residual natural admixture, become equal. However, all three evaporation laws in the (t_i, t_f) region are drastically different. The collimator hindered concentration $c_t(t)$ is immediately going to zero. The relative vapour concentration $c_i(t)$ is much less than the sample concentration $c_r(t)$. This means that evaporation of $_{63}Eu$ out of $_{42}Mo$ and $_{73}Ta$ is additionally hindered, about 50 times (compare $c_i(t_m)$ with $c_r(t_m)$) for implanted $_{63}Eu$ isotopes, e.g., due to separation from surface, and/or initial very fast evaporation without hindrances finished in several seconds and thus remained unobserved. Region (t_f, ∞) shows that natural admixture $_{63}Eu$ evaporation is hindered much stronger (compare $c_i(t_f)$ with $c_r(t_f)$), e.g., due to additional diffusion to surface. Fig. 9 shows also that natural admixture $_{63}Eu$ is considerably more in our $_{42}Mo$ than $_{73}Ta$ samples (compare $c_r(t_f)$ for Mo and Ta).

Mass separated $^{153}_{63}Eu$ and $^{151}_{63}Eu$, implanted in $_{42}Mo$ and $_{73}Ta$, are observed as shown in table 4. Here only the concentrations of the implanted $_{63}Eu$ isotope Δc at $t = 0$ and Δc_m at $t = t_m$ are given:

$$\Delta c = c_r(0) - c_r(t_f), \qquad \Delta c_m = c_r(t_m) - c_r(t_f) \tag{9}$$

together with the corresponding numbers of atoms of the implanted isotope $\Delta\delta$ and $\Delta\delta_m$. And finally the reciprocal sensitivities for implanted $_{63}Eu$ $\Delta c_m\theta_s = (\Delta c_m\chi_s, \Delta c_m\gamma_s, \Delta c_m\gamma_s)$ at $t = t_m$ are shown.

Sensitivities of table 4 are about 50 times worse than those derived from pure Eu experiments in table 2 and from Eu admixture in Sm and Nd experiments in table 3. This means again that the evaporation of Eu implanted in Mo and Ta is additionally hindered about as many times.

8. Minimal nuclide registration amounts

At standard conditions, for a scanning time $t_s = 10$ s ($t_c = 1$ s per channel, 10 channels per scan), high collimation, without additional evaporation hindrances, as it follows from the second row of table 2 and from table 3, the minimal registration amount should be $\gamma_s t_s = 3 \times 10^9$ atom. With additional evaporation hindrances, as it

follows from table 4, this amount might increase to about $\Psi_s t_s$ = 1.5 x 10^{11} atom. An on-line modification is under consideration which should be able to see at standard conditions, but for t_s = 0.1 s per scan (t_c = 0,01 s per channel, 10 channels per scan), high collimation, quite roughly $\Psi_s t_s$ = 3 x 10^8 atom .

Three possibilities are open in this way: Firstly, analysis and investigation of low amount admixtures, natural, implanted and/or obtained as a result of a rare process; Secondly, off-line spectroscopy of stable or radioactive nuclide ground or isomeric states with lifetimes $\gtrsim$ 40 min . For cross sections of about 100 mb, such nuclides can be obtained on the JINR heavy ion accelerators in amounts $\gtrsim$ 6 x 10^{10} atom , but longer living $\gtrsim$ 2.5 x 10^{12} atom; Thirdly, an on-line spectroscopy modification, which should be able to deal with lifetimes $\gtrsim$ 0.1 s . For cross sections of about 100 mb , such nuclides can be obtained on the same accelerators on the level $\gtrsim$ 2.5 x 10^6 atom , but longer living $\gtrsim$ 10^8 atom . In a continuous on-line measurement the minimum registered amount becomes equal to the produced one 3.6 x 10^{10} atom for a time of 24 min.

Acknowledgments

The authors would like to thank Doctors N.I. Tarantin and A.P. Kabachenko for cooperation by performing mass separation and implantation. Thanks are also due to Doctors B.B. Krynetsky, V.A. Mishin and O.M. Stelmakh, Institute of General Physics, Acad. Sci. USSR Moscow, for helping the set up design.

References

1. Jacquinot P., Klapisch R. Rep.Progr.Phys., 1979, 42, p.773.
2. Otten E.W. Nucl.Phys., 1981, A354, p.471c.
3. Otten E.W. In: International School-Seminar on Heavy Ion Physics (Alushta). JINR, D7-83-644, Dubna, 1983, p.158.
4. Nowicki G., Bekk K., Göring S., Hanser A., Rebel H., Schatz G. Phys.Rev., 1978, C18, p.2369.
5. Bekk K., Andl A., Göring S., Hanser A., Nowicki G., Rebel H., Schatz G. Z.Phys., 1979, A291, p.219.
6. Гангрский Ю.П., Маринова К.П., Марков Б.Н., Наджаков Е.Г., Оганесян Ю.Ц., Хан Ген И, Чан Конг Там. Изв. АН СССР сер.физ., 1985, 49, с.2261.

7. Eliel E.R., van Leeuwen K.A.H., Hogervorst W. Phys.Rev., 1980, A22, p.1491.
8. Ahmad S.A., Klempt W., Ekström C., Neugart R., Wendt K. CERN-EP/84-161, Geneva, 1984; submitted to Z.Phys. A.
9. Nadjakov E.G. JINR, E6-86-231, Dubna, 1986; submitted to J.Phys. E Sci.Instr.
10. Несмеянов А.Н. Давление пара химических элементов. Изд. АН СССР, Москва, 1961.
11. Алхазов Г.Д., Барзах А.Е., Берлович Э.Е., Денисов В.П., Дернятин А.Г., Иванов В.С., Жерихин А.Н., Компанец О.Н., Летохов В.С., Мишин В.И., Федосеев В.Н. ЛИАФ АН СССР, 908, Ленинград, 1983.
12. Nadjakov E.G., JINR, E6-86-232, Dubna, 1986; submitted to J.Phys. E Sci.Instr.

Received by Publishing Department
on April 14, 1986.

SUBJECT CATEGORIES OF THE JINR PUBLICATIONS

Index	Subject
1.	High energy experimental physics
2.	High energy theoretical physics
3.	Low energy experimental physics
4.	Low energy theoretical physics
5.	Mathematics
6.	Nuclear spectroscopy and radiochemistry
7.	Heavy ion physics
8.	Cryogenics
9.	Accelerators
10.	Automatization of data processing
11.	Computing mathematics and technique
12.	Chemistry
13.	Experimental techniques and methods
14.	Solid state physics. Liquids
15.	Experimental physics of nuclear reactions at low energies
16.	Health physics. Shieldings
17.	Theory of condenced matter
18.	Applied researches
19.	Biophysics

Гангрский Ю.П., Хан Ген И., Маринова К.П., Марков Б.Н.,
Наджаков Е.Г., Чан Конг Там
E6-86-233

Регистрация низких количеств нуклидов
на лазерном спектрометре с атомным пучком

Исследован лазерный спектрометр, предназначенный для офф-лайн измерения ядерных моментов стабильных и радиоактивных ядер. Его разрешение, селективность, эффективность и чувствительность определены с использованием преимущественно линии 5765.20 Å, а также 6018.19 Å, образцов чистого естественного $^{151,153}_{63}Eu$. Рассмотрены возможности увидеть примеси $_{63}Eu$ в образцах редких земель $_{60}Nd$, $_{62}Sm$, а также масс-сепарированных изотопов $_{63}Eu$, имплантированных в $_{42}Mo$, $_{73}Ta$. Изучено испарение $_{63}Eu$ из этих образцов и возможные помехи для регистрации низких количеств. Таким образом оценены минимальные количества регистрации в идеализированных и реальных условиях.

Работа выполнена в Лаборатории ядерных реакций ОИЯИ.

Препринт Объединенного института ядерных исследований. Дубна 1986

Gangrsky Yu.P., Han Gyong I., Marinova K.P., Markov B.N.,
Nadjakov E.G., Tran Cong Tam
E6-86-233

Low Amount Nuclide Registration by an Atomic Beam Laser Spectrometer

A laser spectrometer designed for off-line nuclear moments determination of stable and radioactive nuclei is investigated. Its resolution, selectivity, efficiency and sensitivity have been determined using mainly the 5765.20 Å line, and also 6018.19 Å, of pure natural $^{151,153}_{63}Eu$ samples. The possibilities to see low amount $_{63}Eu$ admixtures in rare earth samples of $_{60}Nd$, $_{62}Sm$, and also mass separated $_{63}Eu$ isotopes in $_{42}Mo$, $_{73}Ta$ have been considered. The $_{63}Eu$ evaporation from these samples and its possible hindrances to low amount registration have been studied. Thus the minimal registration amounts in idealized and real conditions have been estimated.

The investigation has been performed at the Laboratory of Nuclear Reactions, JINR.

Preprint of the Joint Institute for Nuclear Research. Dubna 1986